

APPROACH TO THE MAPPING OF WATER ENVIRONMENT ON PRESENT MARS – VALIDATION OF POSSIBLE WATER VAPOR EMISSION FROM RECURRING SLOPE LINEAE USING A GCM

T. Kuroda^{1,2} (tkuroda@tohoku.ac.jp), H. Kurokawa³, S. Aoki⁴, H. Nakagawa¹, and M. Kobayashi¹

¹Department of Geophysics, Graduate School of Science, Tohoku University, Sendai, Japan. ²Division for the Establishment of Frontier Sciences, Organization for Advanced Studies, Tohoku University, Sendai, Japan.

³Earth-Life Science Institute, Tokyo Institute of Technology, Tokyo, Japan. ⁴Department of Complexity Science and Engineering, The University of Tokyo, Kashiwa, Japan.

Introduction:

Identification and mapping of the surface and underground water environment on present Mars are important to investigate the existence of life and reserve water resources for future manned missions. Especially, the recurring slope lineae (RSL), dark streaks which appear on steep slopes such as the edge of craters in specific seasons [1], have been noticed as important targets as possible water sources on the surface of Mars. Although the formation mechanisms of RSL are still under discussion, it might be related to the flow of liquid (salty or pure) water. We have simulated the possible water vapor emission and expansion from RSL using a Mars global climate model (MGCM) [2].

Method:

We used a high-resolution coordinate of DRAMATIC (Dynamics, RAdiation, MAterial Transport, and their mutual InteraCtions) MGCM [3] which has a horizontal resolution of ~ 1.1 degrees (~ 67 km) and 53 σ -levels with $\sigma = 0.9995, 0.9998, 0.9955, 0.992, \text{ and } 0.9875$ for the lowest five layers, corresponding to approximately 5, 20, 45, 80, and 125 m above the surface respectively, to well resolve the planetary boundary layer (PBL).

We have performed six scenarios in which the water vapor was emitted from one of five representing grid points which include RSL (in CAP, VM, and SML regions [4], see **Figure 1**), and investigated the qualitative and quantitative transport of water vapor. For each scenario the emission from one RSL (area of 0.1 m^2) was assumed, and the emission rate was defined as 0.1 mm h^{-1} if the surface temperature exceeded 238 K in CAP and VM (assuming salty water), while as 1 mm h^{-1} if the surface temperature exceeded 273 K in SML (assuming pure water) [5].

Table 1 summarizes the emission points and L_s periods for the six scenarios, as well as the surface temperature and pressure conditions during the emission runs (for 20 Sols). Note that the seasonal

and latitudinal variations of dust opacity was defined with ‘MY26 dust scenario’ [6], and the difference of daytime surface temperature between MGCM and MGS-TES observation [6] for MY26 was within 8 K for each scenario.

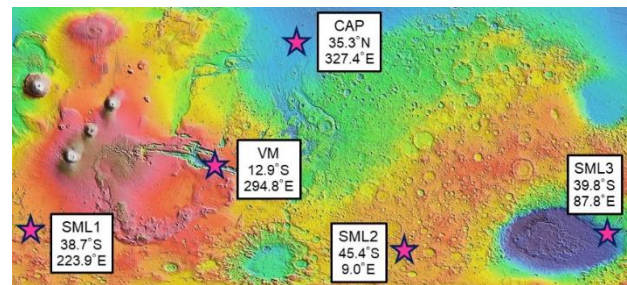


Figure 1. Locations of five emission points (background map: MGS-MOLA data [7]).

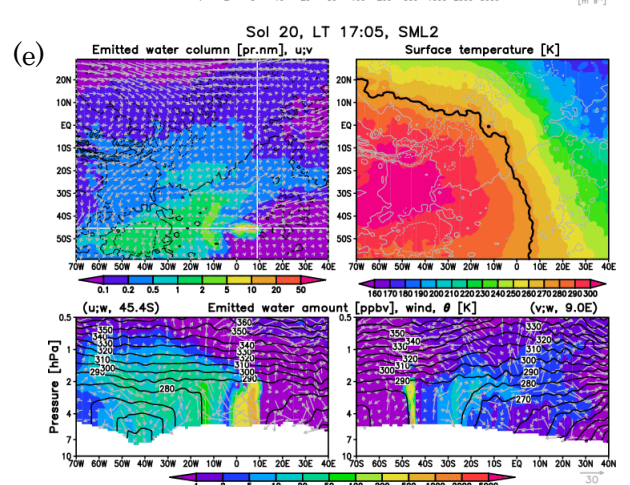
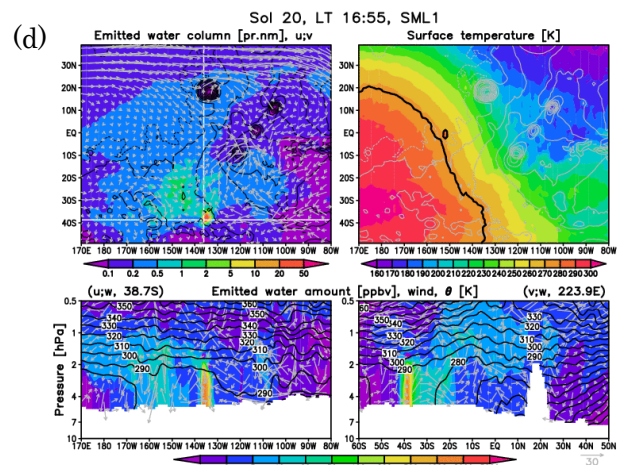
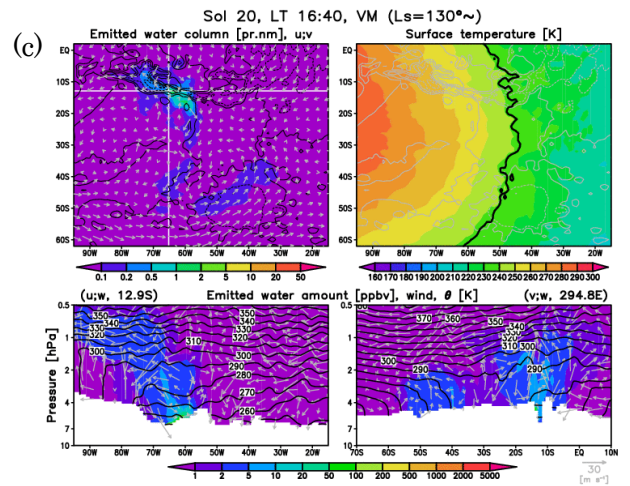
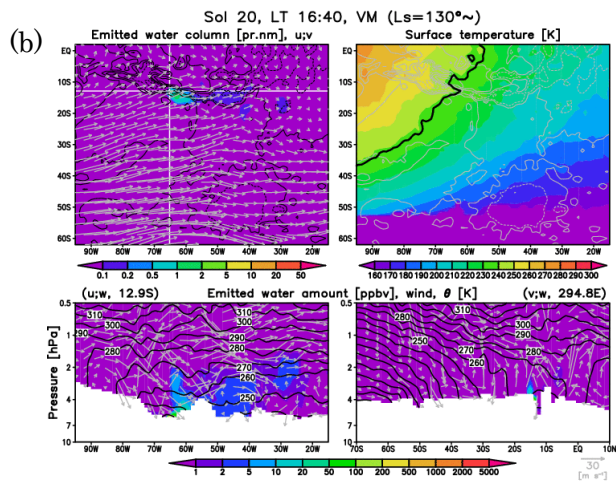
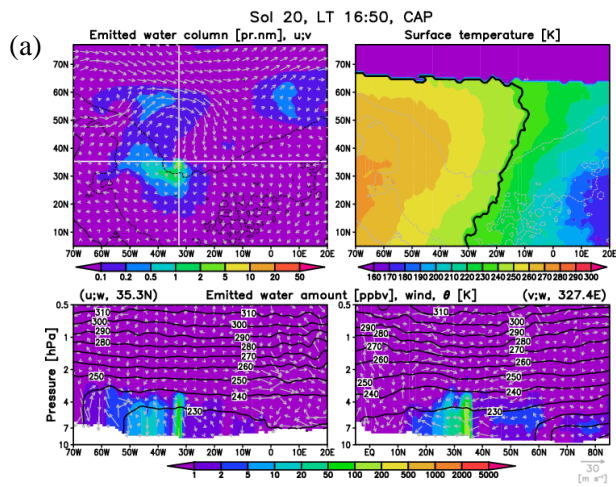
Table 1. Properties of the six scenarios performed in this study.

Point and period	Mean surface pressure during emission [Pa]	Mean emission time length per a Sol [h]
(a) CAP $L_s=50^\circ\sim 59^\circ$	880	9.88
(b) VM $L_s=130^\circ\sim 140^\circ$	625	7.05
(c) VM $L_s=320^\circ\sim 331^\circ$	689	9.85
(d) SML1 $L_s=289^\circ\sim 301^\circ$	513	8.50
(e) SML2 $L_s=289^\circ\sim 301^\circ$	522	8.18
(f) SML3 $L_s=289^\circ\sim 301^\circ$	905	7.68

Results:

Figure 2 shows the snapshots of the simulation results of water vapor emissions from each emission point (corresponding movies are available

in [2]). Our results showed that the column densities of emitted water vapor from one RSL did not exceed 1/300 of the background column density of water vapor (MGS-TES observations in MY26 [8]) for each scenario. Focusing on the movements of emitted water vapor, daytime lifting of water vapor was seen up to ~10 km altitude with the vatically low variations of potential temperatures, depending on the surrounding topographic condition. Note that we did not need to consider the condensation of emitted water vapor, since the water vapor mixing ratio in the PBL did not reach the saturation level for each scenario.



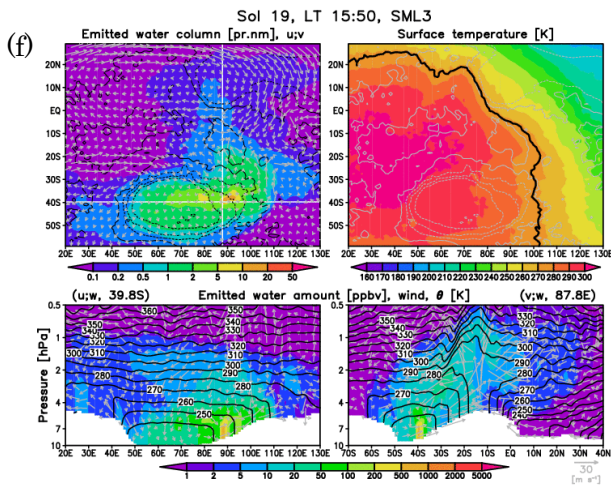


Figure 2. Snapshots of the water vapor distributions emitted from one RSL and atmospheric/surface conditions at the localtime of ~5PM in the 20th sol of simulation. (a)-(f) corresponds to the scenarios listed in **Table 1**.

(top left) Column density of emitted water from one RSL (shades) and the wind field of ~5 m altitude (gray arrows, index is as displayed in the right bottom). The crossover point of two white lines shows the emission point and black contours denote the topography.

(top right) Surface temperature (shades) with the threshold temperature of emission (238 K or 273 K depending on the location, black thick contour). Gray contours denote the topography.

(bottom row) Longitude-altitude (left) and latitude-altitude (right) cross-sections of the mixing ratio of emitted water (shades), potential temperature defined at 6.1 hPa (black contours), and horizontal (zonal or meridional) -vertical wind fields (gray arrows, index is as displayed in the right bottom, vertical velocity is multiplied by 50).

Discussions and future plans:

Our simulation results showed that it would be quite severe to quantitatively detect the emitted water from single RSL by remote-sensing observations even if RSL have a wet origin [2]. However, 475 RSL has been found on Mars, especially concentrative in CAP and VN regions [4], so the actual amount of emission in those regions could be rather higher than the simulation results. Also, it should be noted that the emitted water vapor tended to accumulate in basins and valleys, as indicated in **Figures 2e and 2f**. We plan to perform the simulations using a regional mesoscale model with higher horizontal resolution of topography, which will show the contrast of water vapor distributions affected by the km-scale deviations of topography which could not be represented in our

current simulation.

Moreover, we are implementing the absorption of water vapor by regolith and vertical transport of subsurface water including the emission of underground ice into the MGC with water cycle [9] for the global mapping of water vapor distributions on Mars, in addition to the emissions from RSL. In the presentation we plan show the preliminary results of global water mapping with the effects of regolith.

Acknowledgements:

This work is supported by the Japan Society for the Promotion of Science (JSPS) KAKENHI Grant Numbers 17H06457, 19H01960, 19H05072, 18H04453, 19H00707, 19K03980, 20H04605, 20KK0080, 21H04514, and 21K13976, as well as the Fusion Oriented REsearch for disruptive Science and Technology (FOREST) program of Japan Science and Technology agency (JST). The model runs were performed using the Fujitsu PRIMERGY CX600M1/CX1640M1 (Oakforest-PACS) at the Information Technology Center, The University of Tokyo.

References:

- [1] McEwen, A.S., Dundas, C.M., Mattson, S.S., Toigo, A.D., Ojha, L., Wray, J.J., Chojnacki, M., Byrne, S., Murchie, S.L., Thomas, N., 2014. Recurring slope lineae in equatorial regions of Mars. *Nat. Geosci.* 7, 53–58. <https://doi.org/10.1038/ngeo2014>.
- [2] Kurokawa, H., Kuroda, T., Aoki, S., Nakagawa, H., 2022. Can we constrain the origin of Mars' recurring slope lineae using atmospheric observations? *Icarus* 371, 114688. <https://doi.org/10.1029/2005JE002460>
- [3] Kuroda, T., Medvedev, A.S., Yiğit, E., Hartogh, P., 2015. A global view of gravity waves in the Martian atmosphere inferred from a high-resolution general circulation model. *Geophys. Res. Lett.* 42, 9213–9222. <https://doi.org/10.1002/2015GL066332>
- [4] Stillman, D.E., Michaels, T.I., Grimm, R.E., 2017. Characteristics of the numerous and widespread recurring slope lineae (RSL) in Valles Marineris, Mars. *Icarus* 285, 195–210. <https://doi.org/10.1016/j.icarus.2016.10.025>.
- [5] Altheide, T., Chevier, V., Nicholson, C., Denson, J., 2009. Experimental investigation of the stability and evaporation of sulfate and

chloride brines on Mars. *Earth Planet. Sci. Lett.* 282, 69–78.

<https://doi.org/10.1016/j.epsl.2009.03.002>.

- [6] Christensen, P.R., Bandfield, J.L., Hamilton, V.E., Ruff, S.W., Kieffer, H.H., Titus, T.N., Malin, M.C., Morris, R.V., Lane, M.D., Clark, R.L., Jakosky, B.M., Mellon, M.T., Pearl, J.C., Conrath, B.J., Smith, M.D., Clancy, R.T., Kuzmin, R.O., Roush, T., Mehall, G.L., Gorelick, N., Bender, K., Murray, K., Dason, S., Greene, E., Silverman, S., Greenfield, M., 2001. Mars global surveyor thermal emission spectrometer experiment: investigation description and surface science results. *J. Geophys. Res.* 106, 23823–23871.
<https://doi.org/10.1029/2000JE001370>.
- [7] Smith, M.D., 2008. Spacecraft observations of the Martian atmosphere. *Annu. Rev. Earth Planet. Sci.* 36, 191–219.
<https://doi.org/10.1146/annurev.earth.36.031207.124334>.
- [8] Smith, D.E., Zuber, M.T., Solomon, S.C., Phillips, R.J., Head, J.W., Garvin, J.B., Banerdt, W.B., Muhleman, D.O., Pettengill, G.H., Neumann, G.A., Lemoine, F.G., Abshire, J.B., Aharonson, O., Brown, C.D., Hauck, S.A., Ivanov, A.B., McGovern, P.J., Zwally, H.J., Duxbury, T.C., 1999. The global topography of Mars and implications for surface evolution. *Science* 284, 1495–1503.
<https://doi.org/10.1126/science.284.5419.1495>.
- [9] Kuroda, T., 2017. Simulation of the Water Cycle Including HDO/H₂O Isotopic Fractionation on the Present Mars Using DRAMATIC MGCM. Sixth international workshop on the Mars atmosphere: modelling and observations.
http://www-mars.lmd.jussieu.fr/granada2017/abstracts/kuroda_granada2017_water.pdf